Polymer Chemistry

Degradability, Thermal Stability, and High Thermal Properties in Spiro Polycycloacetals Partially Derived from Lignin

Journal:	*Polymer Chemistry*
Manuscript ID	PY-ART-07-2021-001017
Article Type:	Paper
Date Submitted by the Author:	28-Jul-2021
Complete List of Authors:	Shen, Minjie; University of Houston, William A. Brookshire Dept. of Chemical and Biomolecular Engineering Vijjamarri, Srikanth; University of Houston, William A. Brookshire Dept. of Chemical and Biomolecular Engineering Cao, Hongda; University of Houston, William A. Brookshire Dept. of Chemical and Biomolecular Engineering Solis, Karla; University of Houston, William A. Brookshire Dept. of Chemical and Biomolecular Engineering Robertson, Megan; University of Houston, William A. Brookshire Dept. of Chemical and Biomolecular Engineering

Degradability, Thermal Stability, and High Thermal Properties in Spiro Polycycloacetals Partially Derived from Lignin

Minjie Shen,[a]† Srikanth Vijjamarri, [a]†Hongda Cao,[a] Karla Solis,[a] and Megan L. Robertson[a,b]*

[a]William A. Brookshire Department of Chemical and Biomolecular Engineering, University of Houston, Houston, TX, 77204, United States

[b]Department of Chemistry, University of Houston, Houston, TX 77204, Unites States

† These authors contributed equally to this work

*Corresponding author
Megan Robertson
4726 Calhoun Road
S222 Engineering Building 1
University of Houston
Houston, TX 77204-4004
mlrobertson@uh.edu
713-743-2748

KEYWORDS:

Degradable polymers, hydrolytic degradation, sustainable polymers, lignin, polymer end-of-life, super engineering plastics, polyacetals

Abstract

A series of partially bio-based spiro polycycloacetals was synthesized using lignin-based feedstocks, vanillin and its derivative syringaldehyde, along with pentaerythritol and commercially available co-monomers including 4,4′-difluorobenzophenone (DFP) and bis(4-fluorophenyl) sulfone (DFS). These spiro polycycloacetals displayed high thermal stabilities (degradation temperatures in the range of 343 – 370 °C, as quantified by 5% mass loss) and high glass transition temperatures (in the range of 179 – 243 °C). While DFS-containing polymers were amorphous, DFP-containing polymers were semi-crystalline with high melting temperatures (in the range of 244 – 262 °C). The hydrolytic degradation behavior of one spiro polycycloacetal, derived from vanillin and DFP, was investigated. Importantly, the spiro polycycloacetal was rapidly degraded to small molecules and oligomeric byproducts under acid-catalyzed conditions. This class of spiro polycycloacetals is therefore an important contributor to the development of more easily degradable polymers which also retain sufficiently high thermal properties and thermal stability.

1. Introduction

The derivation of polymers from renewable resources has been of great interest in academia and industry due to their significant applications as eco-friendly materials. Utilization of biobased sources for plastics production minimizes the consumption of petro-chemical reservoirs, limiting industrial dependence on depleting fossil fuel feedstocks.[1-9] The fate of materials in the environment is one of the key considerations in evaluation of the life cycle of polymers.[10, 11] Incorporating labile functional groups into the polymer backbone offers a solution for addressing plastic waste through hydrolytic degradation to small molecule byproducts, which can be subsequently re-used to make new materials.[12-18] In this regard, an increasing effort has been dedicated to providing biomass-derived chemical building blocks to synthesize hydrolytically degradable polymers including polyesters, polyamides, poly(silyl ether)s, polyurethanes, among others.[13, 14, 16-20]

Among the numerous biobased polymers reported, polyacetals are an important class of polymer with remarkable degradation properties and significant potential applications.[4, 21, 22] The presence of a cleavable acetal unit in the polymer backbone permits rapid degradation under acid-catalyzed hydrolysis.[21-26] Polyacetals have been synthesized from renewable feedstocks, such as starch [27] and cellulose.[28] Among these renewable feedstocks, vanillin, a lignin-derived compound, and its derivative, syringaldehyde, have gained much popularity recently.[2, 29-32] The presence of hydroxyl and aldehyde functional groups, as well as highly aromatic structures, on these lignin-based molecules make them prime candidates as chemical feedstocks for high performance, biobased polyacetals.[2, 31, 32]

The thermal stabilities and thermal transitions of synthetic polymers are major criteria to determine their potential applications.[33] Polymers such as poly(arylene ether)s, poly(ether ether

ketone), and polyphenylsulfones are used in super engineering plastics due to their high glass transition temperatures (T_g), which are typically greater than 150 °C.[34-36] However, the majority of these high T_g super engineering plastics are non-degradable and synthesized from petrochemical feedstocks.[37, 38] It is therefore of much interest to synthesize high-T_g polymers from biobased feedstocks with enhanced degradation properties. In the case of polyacetals, the majority of literature studies have involved linear polyacetals, which exhibited low thermal degradation temperatures, low T_g, and poor chemical resistance, which limits their engineering applications.[27, 39-42] To overcome these limitations, researchers have focused on the design of polyacetals with structurally rigid backbones. In this regard, incorporation of cycloacetal and spiro cycloacetal units into the polymer backbone has gained much interest in the literature.[31, 32, 43-45] The structural rigidity in the polymer backbone increased the T_g relative to non-cyclic polyacetals, though the thermal degradation temperatures were not greatly enhanced.[31, 32, 44, 45] Thus, designing and developing polyacetals with inherent degradability, high T_g, and superior thermal stability is a challenging but extremely significant problem.

Herein we describe the synthesis and characterization of spiro polycycloacetals utilizing bioaromatic hydroxyaldehydes, polyols, and aromatic sulfonates or benzophenone. Notably, the incorporation of aromatic sulfonates or benzophenone into the polymer backbone, along with bioaromatic aldehydes, increased the aromaticity and rigidity of polymer backbone, which further improved the polymer thermal stability as well as T_g.[36] To our knowledge, these are the first examples of bioaromatic-based spiro polycycloacetals with T_g values up to 243°C, melting points up to 262°C, and thermal degradation temperatures (quantified as 5% mass loss) up to 370 °C. We also demonstrate their rapid hydrolytic degradation in acidic media. The hydrolytic degradation behavior of one spiro polycycloacetal, derived from vanillin and 4,4′-difluorobenzophenone (DFP),

was quantified in various acidic solvents; the polymer showed the fastest degradation behavior in acidic acetone and degraded completely to small molecule and oligomeric byproducts within 10 h.

2. Experimental Methods

2.1 Materials

All chemicals were purchased from Sigma-Aldrich unless otherwise noted and were used as received: *p*-hydroxybenzaldehyde (vanillin, ≥97%, FG), 3,5-dimethoxy-4-hydroxybenzaldehyde (syringaldehyde**,** ≥98%, FG), difluorobenzophenone (DFP, 99%), bis(4-fluorophenyl) sulfone (DFS, 99%), 2,2-bis(hydroxymethyl)-1,3-propanediol (pentaerythritol, 99%), *p*-toluene sulfonic acid monohydrate (*p*-TSA.H_2O, ACS reagent, ≥98.5%), N,N-dimethylformamide (DMF, anhydrous, 99.8%), sodium bicarbonate ($NaHCO_3$, ACS reagent, ≥99.7%), potassium carbonate (K_2CO3, 9.995% trace metals basis), 18-crown-6 (≥99.0%), dimethyl sulfoxide-d_6 (*d*-DMSO, 99.9 atom % D, purchased from Cambridge Isotope Laboratories), deuterium oxide (D_2O, 99.9 atom % D), acetone-d_6 (99.9 atom % D), dimethylsulfoxide (DMSO, anhydrous, ≥99.9%), petroleum ether (ACS reagent), methanol (HPLC, ≥99.9%), acetone (ACS reagent, ≥99.5%), ethyl acetate (ACS reagent, ≥99.5%), and 1,2,4,5-tetramethylbenzene (ACS reagent, ≥98%), acetonitrile (HPLC, ≥99.9%).

2.2 Monomer Synthesis

Synthesis of 4,4'-(2,4,8,10-tetraoxaspiro[5.5]undecane3,9-diyl)bis(2-methoxyphenol) (VPA): The synthesis of VPA followed previously reported protocols.[31] Two eqv. of vanillin (40.0 g) and 1 eqv. of pentaerythritol (18.0 g) were added to a dry 500 mL round bottom flask equipped with a mechanical stir bar and a Dean–Stark trap, followed by the addition of a catalyst,

p-TSA.H_2O (1.12 g, 2 wt% of the total weight of vanillin and pentaerythritol), at room temperature. DMF (165 mL) was then added as the solvent and petroleum ether (180 mL) as the water-removing solvent (in which the petroleum ether was boiled continuously to remove produced water, and subsequently condensed back into the reaction flask). The reaction flask was connected to a reflux condenser and then heated at 90 °C overnight (18-20 h). After the reaction, the flask was cooled to room temperature and the reaction mixture was transferred into a 1 L $NaHCO_3$ aqueous solution (3 wt. %) and filtered using a Büchner funnel (equipped with filter paper) attached to a 1 L vacuum flask. The resulting product was washed with 100 mL of distilled water 4-5 times. The purified VPA monomer was dried at 80 °C overnight (18-20 h). 36 g of product was obtained as a white solid (yield: 67.8%).

Synthesis of 4,4'-(2,4,8,10-tetraoxaspiro[5.5]undecane3,9-diyl)bis(2,6-dimethoxyphenol) (SPA): The synthesis and purification of SPA followed the same procedures as that of VPA. Syringaldehyde (48.0 g) was used in place of vanillin. 39 g of SPA monomer was obtained as a white solid (yield: 63.8%).

2.3 Polymer Synthesis

Synthesis of VPA-DFP: VPA (8.08 g, 20 mmol) and DFP (4.36 g, 20 mmol) monomers were added to a dry single-neck round bottom flask, equipped with a mechanical stir bar and a Dean–Stark apparatus, followed by 25.70 mmol of K_2CO_3 (3.45 g). Next, 1.02 mmol (0.27 g) of 18-crown-6 (0.05 molar equivalent to diol, i.e., VPA) was added to the flask, followed by the addition of 100 mL of DMSO under nitrogen flow. The reaction mixture was heated for 24 h at 155 °C under nitrogen.[36] The round bottom flask was then cooled to room temperature and precipitated into a 1 L H_2O/methanol mixture (50/50 by volume). The precipitated polymer was filtered using a Büchner funnel (equipped with filter paper) attached to a 1 L vacuum flask and

slowly washed with 100 mL of distilled water followed by methanol (15 mL), acetone (15 mL), and ethyl acetate (15 mL). The extracted polymer was dried under vacuum at 80 °C overnight (20-24 h). 9.5 g of VPA-DFP was obtained as the final product (yield: 77.6%).

Synthesis of SPA-DFP: Polymer synthesis and purification procedures followed that described above for VPA-DFP, with the exception that the following monomers were used: SPA (9.3 g, 20 mmol) and DFP (4.37 g, 20 mmol). 9.2 g of SPA-DFP was obtained as the final product (yield: 68.4%).

Synthesis of VPA-DFS: Polymer synthesis and purification procedures followed that described above for VPA-DFP, with the exception that the following monomers were used: VPA (8.08 g, 20 mmol) and DFS (5.09 g, 20 mmol). 10.5 g of VPA-DFS was obtained as the final product (yield: 80.9%).

Synthesis of SPA-DFS: Polymer synthesis and purification procedures followed that described above for VPA-DFP, with the exception that the following monomers were used: SPA (9.3 g, 20 mmol) and DFS (5.09 g, 20 mmol). 11.2 g of SPA-DFS was obtained as the final product (yield: 79.1%).

2.4 Monomer and Polymer Characterization

Nuclear magnetic resonance (NMR): ^{1}H NMR (400, 500, 600 MHz), ^{13}C NMR (600 MHz), DEPT (600 MHz), COSY (600 MHz) and HMQC (600 MHz) experiments were conducted using a JEOL ECA-400 spectrometer with deuterated solvents. For analysis of synthesized monomers and polymers, *d*-DMSO was used. For analysis of polymer degradation products, *d*-acetone, *d*-DMSO, and D_2O were used. Chemical shifts were referenced to the residual protonated

solvent resonance (^{1}H NMR: 2.50 ppm for DMSO, 4.80 ppm for H_2O, and 2.04 ppm for acetone. ^{13}C NMR: 39.5 ppm for DMSO and 29.8 ppm for acetone).

Liquid chromatography-mass spectrometry (LC-MS): LC-MS measurements were conducted using an Agilent 6545 QTOF/LC-MS System. The instrument was equipped with a Dual AJS ESI source. The mass range was 60-1,700 m/z. The mobile phase was a mixture of 95% methanol / 5% water, containing 0.1% formic acid, and the flow rate is 0.2 ml/min. The degradation products were dissolved in acetonitrile and the concentration of the solution was 10 μg ml^{-1} prior to injection into the QTOF/LC-MS. The injection volume was 5 μL.

Gel permeation chromatography (GPC): GPC measurements were performed using a Tosoh high performance GPC system (HLC-8320), equipped with an auto injector, a dual differential refractive index (RI) detector, and TSKgel HHR columns connected in series (7.8x300mm G5000HHR, G4000HHR, and G3000HHR), using DMF (Fisher Scientific, Alfa Aesar, HPLC grade, >99.7%, containing 1 g/L LiBr) as the eluent at a flow rate of 1.0 mL/min at 60 °C. Samples were run in triplicate with 100 μL injection volume. Number-average and weight-average molecular weights (M_n and M_w, respectively) and dispersity ($Đ$) were calculated using polystyrene standards with molecular weights ranging from 0.5 to 2.9×10^3 kg/mol provided by Tosoh Science.

Differential scanning calorimetry (DSC): DSC thermograms were collected using a TA Instruments Q2000 differential scanning calorimeter, under 50 mL/min nitrogen flow, and the instrument was calibrated using an indium standard. Samples were encapsulated in hermetic pans, equilibrated at -50 °C, and subjected to a heat – cool – heat cycles from -50 to 300 °C at a rate of 10 °C/min. Melting temperature (T_m) was determined from the peak minimum in the first heating cycle and T_g was identified as the inflection point in the second heating cycle.

Thermogravimetric analysis (TGA): TGA experiments were performed using a TA Instruments Q500 analyzer with alumina sample cups. The samples were heated from 25 – 800 °C at a rate of 10 °C min^{-1} under nitrogen environment. Advantage software was used to analyze the TGA data.

Contact angle measurements: VPA-DFP was coated on silicon wafer using flow coating at 3 cm/s. The silicon wafer was cleaned using a chemical wash and UV-treated for 2 h to remove any contaminants prior to polymer coating. For each silicon wafer, 10 µL solution (5 wt% VPA-DFP in DMSO) was added for flow coating. The silicon wafer was preheated to 90 ^{0}C for better evaporation of DMSO and coating efficiency. Then, contact angles were measured using an OCA 15EC video-based optical contact angle measuring instrument at ambient temperature. The SCA 20 software was used to record the water contact images. 5 µL of the solutions used in degradation experiments (acidic *d*-acetone, *d*-DMSO or D_2O) were deposited onto 3 different positions on the silicon wafer coated with VPA-DFP polymer.

Polymer degradation experiments: Degradation studies were performed in NMR tubes at room temperature. A clean and dry NMR tube was loaded with 10 mg of VPA-DFP and 2.24 mg of 1,2,4,5-tetramethylbenzene (internal standard, for quantitative analysis), followed by the addition of 0.6 mL of deuterated solvent (*d*-acetone, *d*-DMSO or D_2O). The molar ratio of polymer and internal standard used in the degradation study was 1:1. The concentration of the internal standard was 0.0279 mol/L. A homogeneous mixture was formed when *d*-DMSO was added to the polymer, as it is soluble in DMSO. A non-homogeneous mixture was formed when *d*-acetone and D_2O were added to the polymer, as the polymer is not soluble in these solvents. The NMR tube was then charged with 5 µL of HCl solution in H_2O (35 wt%) to promote acid-catalyzed hydrolysis, with a final acid concentration of 0.1 M. ^{1}H NMR data were obtained at different time

intervals in all three solvents and GPC data were obtained at different time intervals in acidic *d*-acetone. At 24 h of total degradation time in acidic *d*-acetone, additional characterization experiments were performed: ^{13}C and 2D NMR, GPC, and LC-MS.

To prepare the samples for GPC measurements, the solvent (*d*-acetone) was removed using a rotary evaporator, and the collected degradation products were dissolved in hexane, followed by extraction using DMF to remove remaining acid and salts prior to injecting in the GPC column. To prepare the samples for LC-MS measurements, the solvent (*d*-acetone) was removed using a rotary evaporator, and the collected degradation products were dissolved in hexane, followed by extraction using acetonitrile to remove remaining acid and salts prior to injecting in the LC-MS column.

3. Results and Discussion

3.1 Synthesis of Spiro Acetal Diol Monomers and Spiro Polycycloacetals

The synthesis of spiro polycycloacetals followed a two-step process, including synthesis of bifunctional spiro acetal diol monomers and step-growth polymerization. Bifunctional spiro acetal diol monomers, VPA and SPA, were synthesized using the biogenic hydroxyaldehydes vanillin and syringaldehyde, respectively, along with pentaerythritol and *p*-TSA.H_2O as the catalyst (**Scheme 1**). Although the synthesis of VPA was previously reported and utilized to prepare polycycloacetals,[31] to our knowledge the synthesis of SPA has not been demonstrated. These monomers were characterized using ^{1}H and ^{13}C NMR (**Figures 1, S1, and S2**). Disappearance of a characteristic aldehyde (-CHO) peak observed in the starting material (vanillin or syringaldehyde) at 9.92-9.98 ppm and appearance of a characteristic -CH peak of the spirocycloacetal unit at 5.34-5.37 ppm in ^{1}H NMR confirmed the formation of the monomers VPA and SPA (**Figure 1a and S1a**).

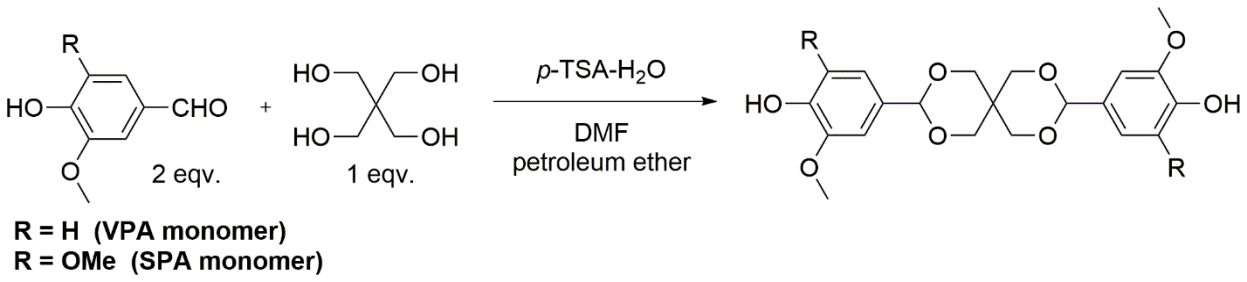

Scheme 1: Synthesis of spiro acetal monomers.

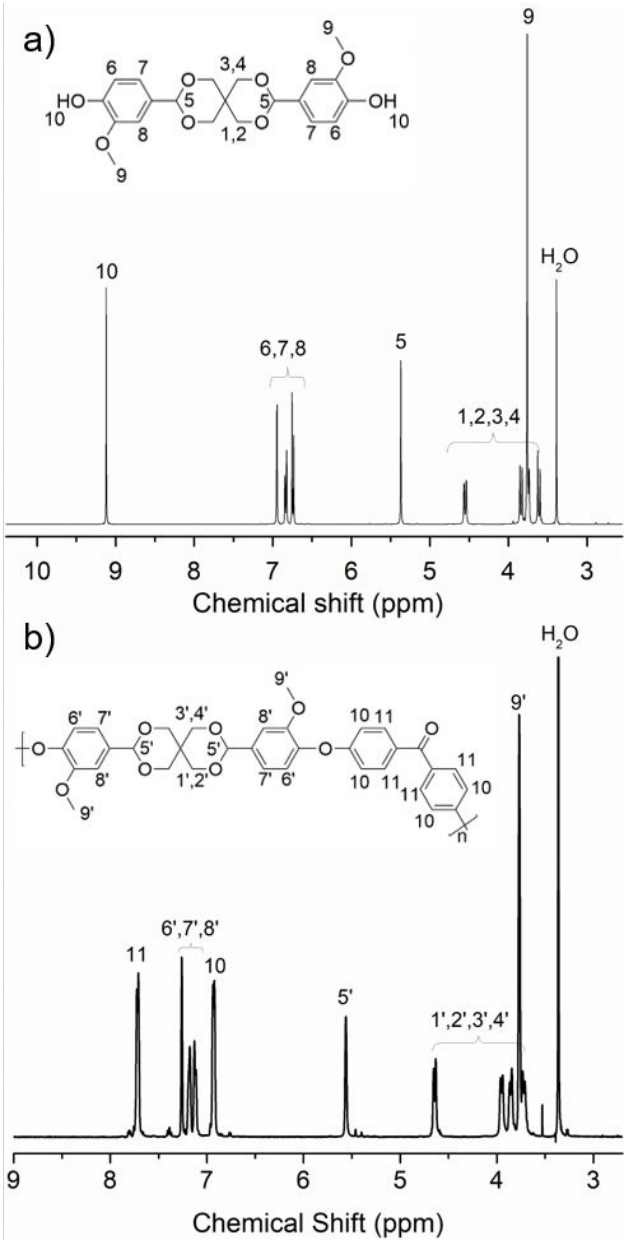

Figure 1: ^{1}H NMR of (a) VPA monomer and (b) VPA-DFP polymer (in *d*-DMSO). Additional ^{1}H and ^{13}C spectra are provided in Figures S1 and S2.

Spiro polycycloacetals were synthesized using monomers VPA or SPA with a co-monomer (either DFP or DFS) through step-growth polymerization in DMSO at 155 °C, employing K_2CO_3 as the catalyst (**Scheme 2**). The reaction progress was monitored using ^{1}H NMR (**Figure 1b**). As the polymerization proceeded, disappearance of peaks associated with hydroxyl groups in the VPA

monomer at 9.12 ppm (peak 10 in **Figure 1a**) and shifting of the characteristic -CH peak from 5.37 ppm in VPA monomer **(**peak 9 in **Figure 1a)** to 5.56 ppm in VPA-DFP **(**peak 9' in **Figure 1b)**, as well as shifting of peaks associated with aromatic hydrogens from 6.75-6.95 ppm in the VPA monomer **(**peaks 6-8 in **Figure 1a)** to 7.11-7.26 ppm in VPA-DFP **(**peaks 6'-8' in **Figure 1b)** confirmed the depletion of VPA monomer and formation of VPA-DFP polymer. In addition, appearance of peaks associated with the phenyl group in the co-monomer (DFP or DFS) in the aromatic region (at 6.94 and 7.72 ppm) confirmed the incorporation of co-monomer into the polymer chain. The formation of other spiro polycycloacetals (VPA-DFS, SPA-DFP, and SPA-DFS) were also confirmed based on the NMR analysis and the detailed ^{1}H and ^{13}C NMR data are presented in **Figures S1 and S2**.

GPC data quantified the number-average molecular weight (M_n) in the range of 4-16 kg/mol and dispersities (Đ) in the range of 1.8-2.8 (**Table 1**), with GPC chromatographs shown in **Figure 2**. Interestingly, VPA-derived polymers showed higher molecular weights than corresponding SPA-derived polymers (**Table 1**), when synthesized under the same conditions. These results suggest that the structurally more rigid syringaldehyde-derived monomer (SPA) exhibited less reactivity than the less rigid vanillin-derived monomer (VPA). Comparatively, polymers synthesized from the DFS co-monomer exhibited higher molecular weights than corresponding polymers synthesized from the DFP co-monomer (**Table 1**).

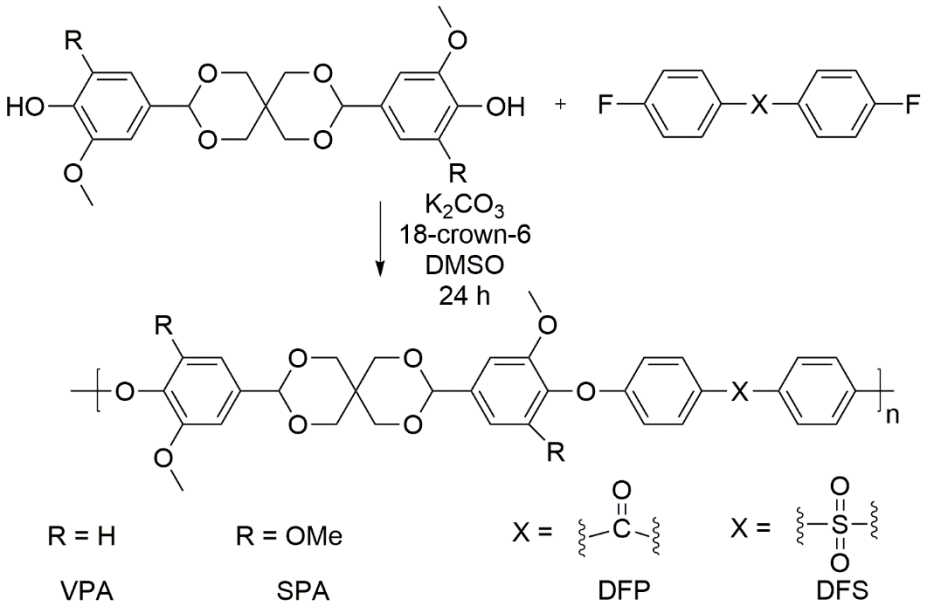

Scheme 2: Synthesis of spiro polycycloacetals.

Table 1: Polymer characteristics[a]

Polymer	M_n (kg/mol)	M_w (kg/mol)	Đ
VPA-DFP	7.3	12.8	1.76
VPA-DFS	16.1	44.7	2.78
SPA-DFP	3.7	7.8	2.12
SPA-DFS	8.9	22.0	2.47

[a]Determined with GPC using polystyrene standards.

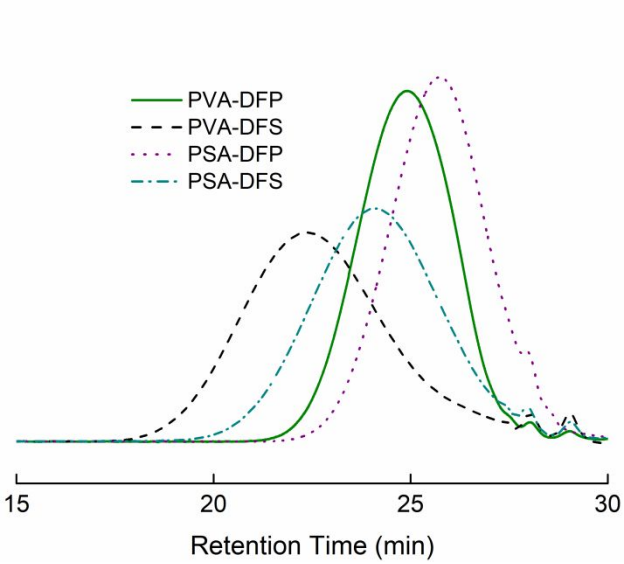

Figure 2: GPC chromatographs of polycycloacetals.

3.2 Elevated Thermal Transitions and Stability of Spiro Polycycloacetals

The thermal degradation temperatures of spiro polycycloacetals were evaluated using TGA, conducted from 25 – 800 °C under an inert (Argon) atmosphere. Irrespective of the molecular weight and polymer backbone, all polymers displayed a multi-stage decomposition profile (**Figure 3**). The polymers exhibited $T_{-5\%}$ (the temperature at which 5% weight loss was observed) in the range of 343 – 370 °C, $T_{-50\%}$ (the temperature at which 50% weight loss was observed) in the range of 460 – 506 °C, and T_{max} (the temperature at which the derivative weight % was maximum) in the range of 425 – 537 °C (**Table 2**), which are significantly higher than that previously reported for other cyclic and spiro polycycloacetals (e.g., $T_{-5\%}$ was previously reported in the range of 210 – 349 °C).[32, 44, 45]

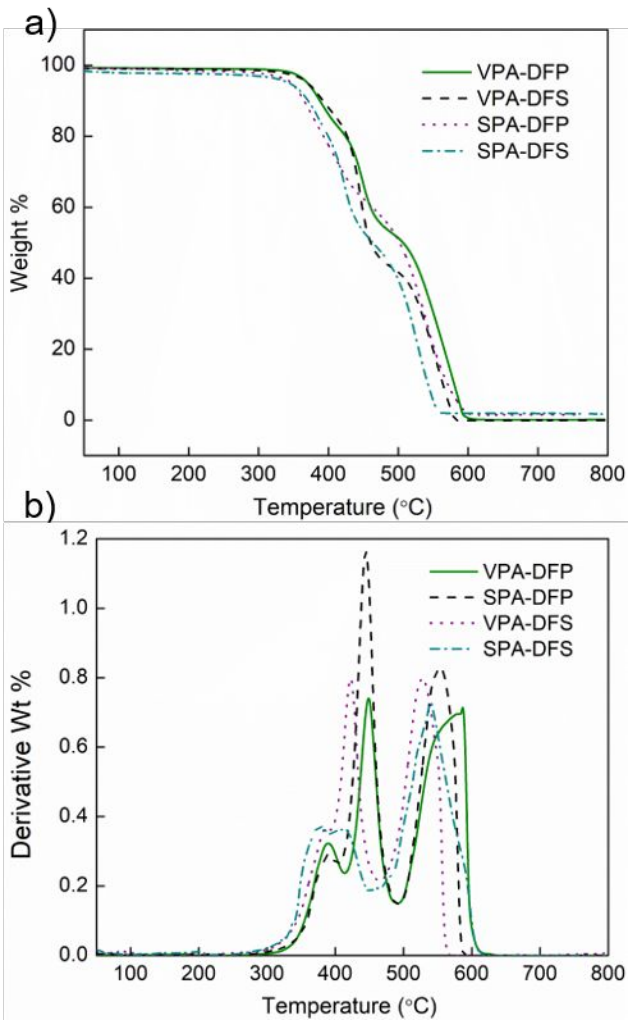

Figure 3: (a) Weight % and (b) derivative weight % as a function of temperature obtained from spiro polycyclocacetals using TGA.

Table 2: Thermal properties of spiro polycycloacetals

Polymer	T_g (°C)	T_m (°C)	$T_{-5\%}$ (°C)	$T_{-50\%}$ (°C)	T_{max} (°C)	Final residual %
VPA-DFP	179	262	370	506	448	1.5
VPA-DFS	217	NA[a]	347	501	445	0
SPA-DFP	193	244	370	461	425	1.6
SPA-DFS	243	NA[a]	343	460	537	1.7

[a] Not applicable (NA): melting was not observed in these polymers.

DSC thermograms obtained from the first and second heating cycles for VPA-DFP are shown in **Figure 4** and that of the other polymers are shown in **Figure S3**. The thermal properties (T_g, T_m) of all of the polymers are listed in **Table 2**. The T_g values of these polymers were in the range of 179-243 °C, significantly higher than that reported previously for spiro polycycloacetals (in the range of 57 – 159 °C).[32, 44, 45] Interestingly, a T_m was observed for the two spiro polycycloacetals synthesized with the DFP comonomer (VPA-DFP and SPA-DFP), but crystallization was not observed during the cooling cycle; these combined results suggest these are semi-crystalline polymers with relatively slow crystallization rates. Polymers synthesized with the DFS comonomer (VPA-DFS and SPA-DFS) did not exhibit crystallization or melting.

As noted above, these polymers exhibited higher T_g values than that of other cyclic and spiro polycycloacetals reported in literature.[32, 44, 45] Incorporating the sterically hindered aromatic co-monomer, DFP or DFS, into the polyacetal backbone thus increased the T_g, which is similar to behavior observed in other super engineering plastics.[36] Since SPA is more structurally rigid than VPA due to the presence of an additional methoxy group, the T_g's of SPA-based polymers were greater than that of the corresponding VPA-based polymers (**Table 2**). Similarly, polymers synthesized using the DFS co-monomer displayed higher T_g's than the corresponding polymers synthesized from the DFP co-monomer, due to the higher rigidity of DFS (**Table 2**).

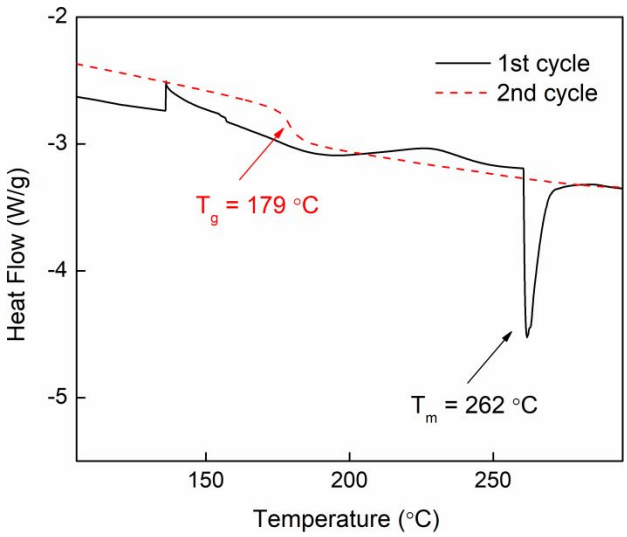

Figure 4: Heat flow vs. temperature obtained for VPA-DFP using DSC, shown for the first and second heating cycles.

3.3 Identifying Hydrolytic Degradation Products of VPA and VPA-DFP in Acidic d-Acetone

We performed degradation studies on VPA and VPA-DFP in acidic *d*-acetone (at 0.1 M HCl; 0.6 mL *d*-acetone containing 5 µL of 35 wt% aqueous HCl solution) and monitored the degradation progress using NMR, LC-MS, and GPC. Here we first discuss the identification of degradation products at the end of the degradation process (after 24 h in acidic *d*-acetone for VPA-DFP and 1 h in acidic *d*-acetone for VPA monomer). In the subsequent section, we will present data which track the formation of degradation products over time.

We begin with the degradation behavior of the VPA monomer. Since VPA is soluble in acetone, an initial NMR spectrum was taken before degradation and compared with that obtained after 1 h degradation time (**Figure S4** and **Scheme S1**). The VPA monomer was completely degraded in acidic *d*-acetone in less than 1 h and produced vanillin as the major degradation product. The characteristic -CH peak observed in VPA at 5.40 ppm ^{1}H NMR (labeled peak 5 in **Figure S4a**) disappeared after 1 h, accompanied by the appearance of peaks associated with

vanillin including the -CHO peak at 9.81 ppm, two sets of aromatic proton peaks at 6.98 and 7.45 ppm, and an -OCH_3 peak at 3.90 ppm (labeled peaks 1, 2/3/4, and 5 in **Figure S4b**, respectively), confirming cleavage of acetal groups of VPA under acidic conditions. In addition, appearance of the -CH_2 peak of pentaerythritol, a byproduct, at 3.75 ppm (labeled peak 7 in **Figure S4b**) confirms the cleavage of acetal groups in the VPA monomer. The appearance of peaks related to vanillin and pentaerythritol clearly suggest that acetal groups are cleavable under acidic conditions. These results led us to perform degradation experiments of VPA-DFP under acidic conditions.

We now discuss the polymer degradation behavior in acidic *d*-acetone. A full discussion of 2D NMR analyses (**Figures S5-S11**) is provided in the ESI. VPA-DFP is not soluble in acetone and thus only the presence of degradation products and oligomers small enough to be solubilized could be monitored with ^{1}H NMR. We consider the proposed small molecule degradation products which could be formed through acid-catalyzed cleavage of acetal groups summarized in **Scheme 3**. Two neighboring repeat units are highlighted in **Scheme 3**. If both spiro acetals groups fully hydrolyze, the degradation product labeled DP-1 will be formed. If both spiro acetal groups only partially hydrolyze, the degradation product labeled DP-3 will be formed. Finally, if one spiro acetal group fully hydrolyzes and one spiro acetal group partially hydrolyzes, the degradation product labeled DP-2 will be formed. Additionally, full hydrolysis of spiro acetal groups will produce pentaerythritol as a byproduct. We note that if there are unhydrolyzed segments of the polymer, oligomers may be formed with these end-group structures.

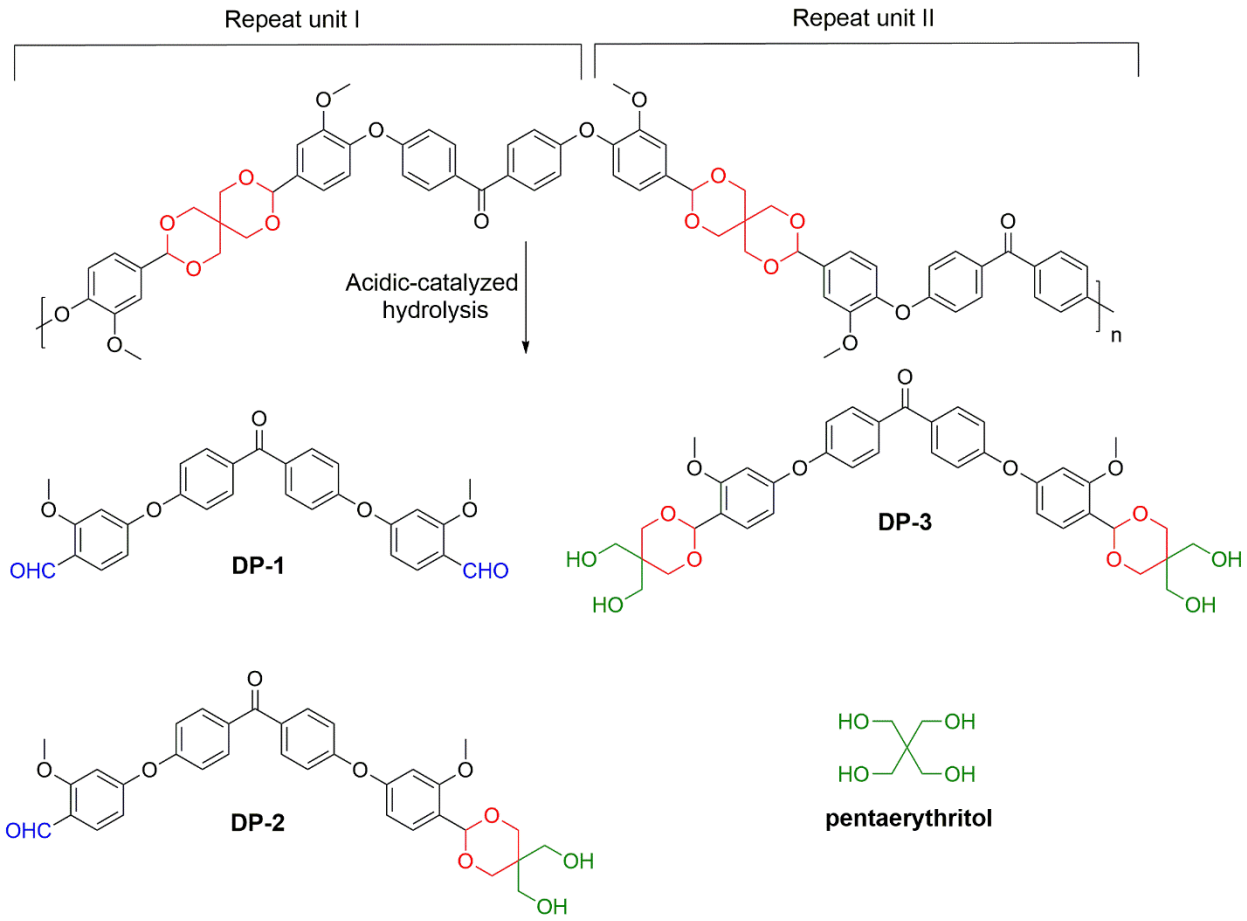

Scheme 3: Proposed degradation pathway of the spiro polycycloacetal VPA-DFP in an acidic medium, including probable degradation products. DP: degradation product.

In order to confirm the presence of the four proposed degradation products in **Scheme 3**, ^{1}H, ^{13}C and 2D NMR data were obtained for VPA-DFP after 24 h in acidic *d*-acetone (**Figures 5 and S5 – S11**). Refer to the discussion in the ESI for more details on the peak assignments, obtained through 2D NMR analyses. The presence of fully hydrolyzed acetal groups (found on DP-1 and DP-2 in **Scheme 3**) was identified through the appearance of the -CHO peak at 10.01 ppm in ^{1}H NMR and 191.7 ppm in ^{13}C NMR (labeled peak 2 in **Figures 5 and S7**, respectively). The partially hydrolyzed acetal groups (on DP-2 and DP-3 in **Scheme 3**) are observed through appearance of the -CH groups at 5.48 and 5.58 ppm in ^{1}H NMR and 102 ppm in ^{13}C NMR (labeled peak 10 in **Figures 5 and S7**, respectively), as well as -OH groups at 4.7 ppm in ^{1}H NMR (labeled

peak 12 in **Figure 5**). We note that the -CH peaks on DP-2 and DP-3 (peak 10 in **Figure 5**) are not expected to be distinguishable; we hypothesize that two peaks are observed in this region due to the presence of H-D exchange, thus shifting the peak slightly. The presence of pentaerythritol is observed through the appearance of the -CH_2 peak at 3.5 ppm in ^{1}H NMR (labeled peak 11 in **Figure 5**) and 32 ppm in ^{13}C NMR (labeled peak 18 in **Figure S7**). Some peaks associated with aromatic protons (labeled as 6-7 and 6'-7'observed in the region of 6.9 – 7.8 ppm in **Figure 5**), are not distinguishable among the three degradation product structures (DP-1, DP-2, and DP-3). However, other aromatic protons (labeled as 3', 4', 5' in **Figure 5**) are shifted due to proximity to the partially hydrolyzed acetal structure. The detailed NMR analyses (discussed further in the ESI) therefore support the conclusion that the acid-catalyzed hydrolysis of VPA-DFP resulted in the four degradation products shown in **Scheme 3**, potentially accompanied by oligomers with the same functionalities.

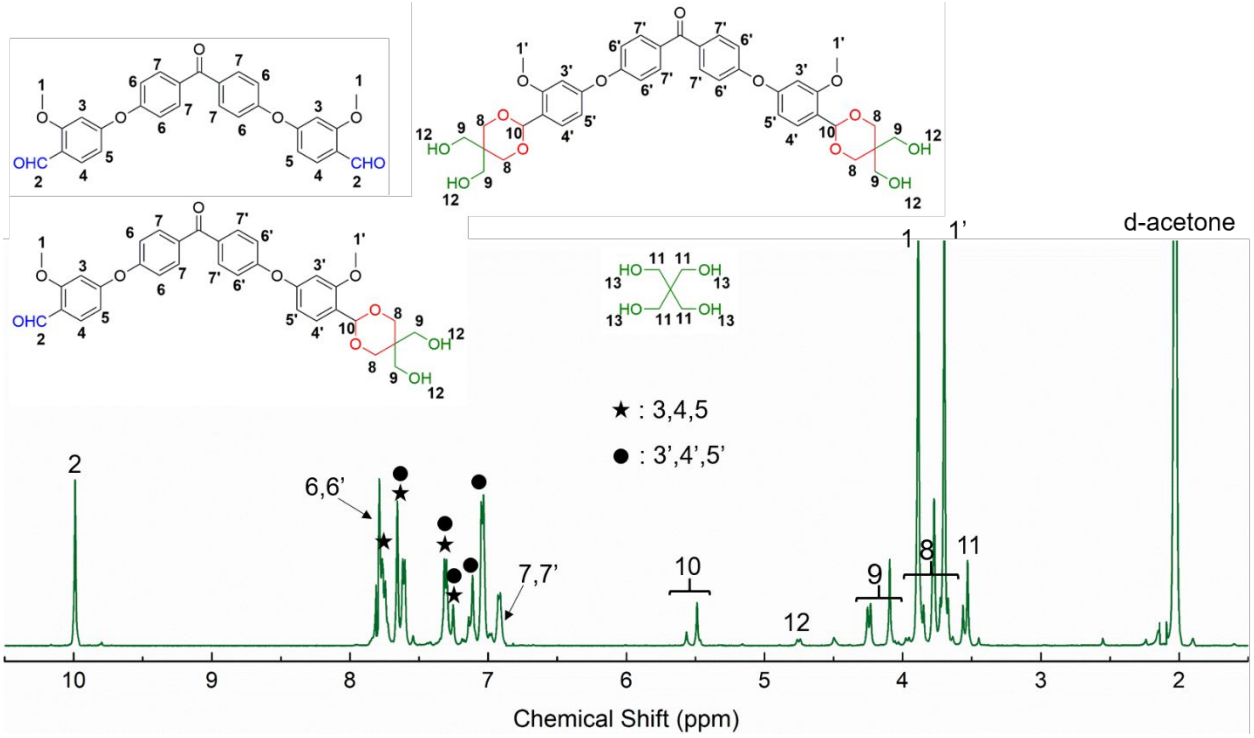

Figure 5: ^{1}H NMR data obtained from the acid-catalyzed hydrolysis of VPA-DFP in *d*-acetone/HCl (0.1 M HCl, pH 1) at room temperature after 24 h. Degradation experiments were conducted in 0.6 mL *d*-acetone containing 5 µL of 35 wt% aqueous HCl solution.

We used LC-MS to further confirm the identification of degradation products (**Figure 6**). Peaks were observed at m/z of 483 (**Figure 6a**), 601 (**Figure 6b**), 719 (**Figure 6c**), and 137 (**Figure 6d**), confirming the presence of DP-1, DP-2, DP-3, and pentaerythritol, respectively, as the degradation products (products were bound with H^+ and/or Na^+ ions as described in **Table 3**). The respective peak intensities showed that the majority degradation products were DP-1 and pentaerythritol, and only a small amount of DP-2 and DP-3 existed in the degradation product mixture after 24 h. The presence of oligomeric species could not be detected as their size would be outside the accessible range of m/z values for this LC-MS instrument.

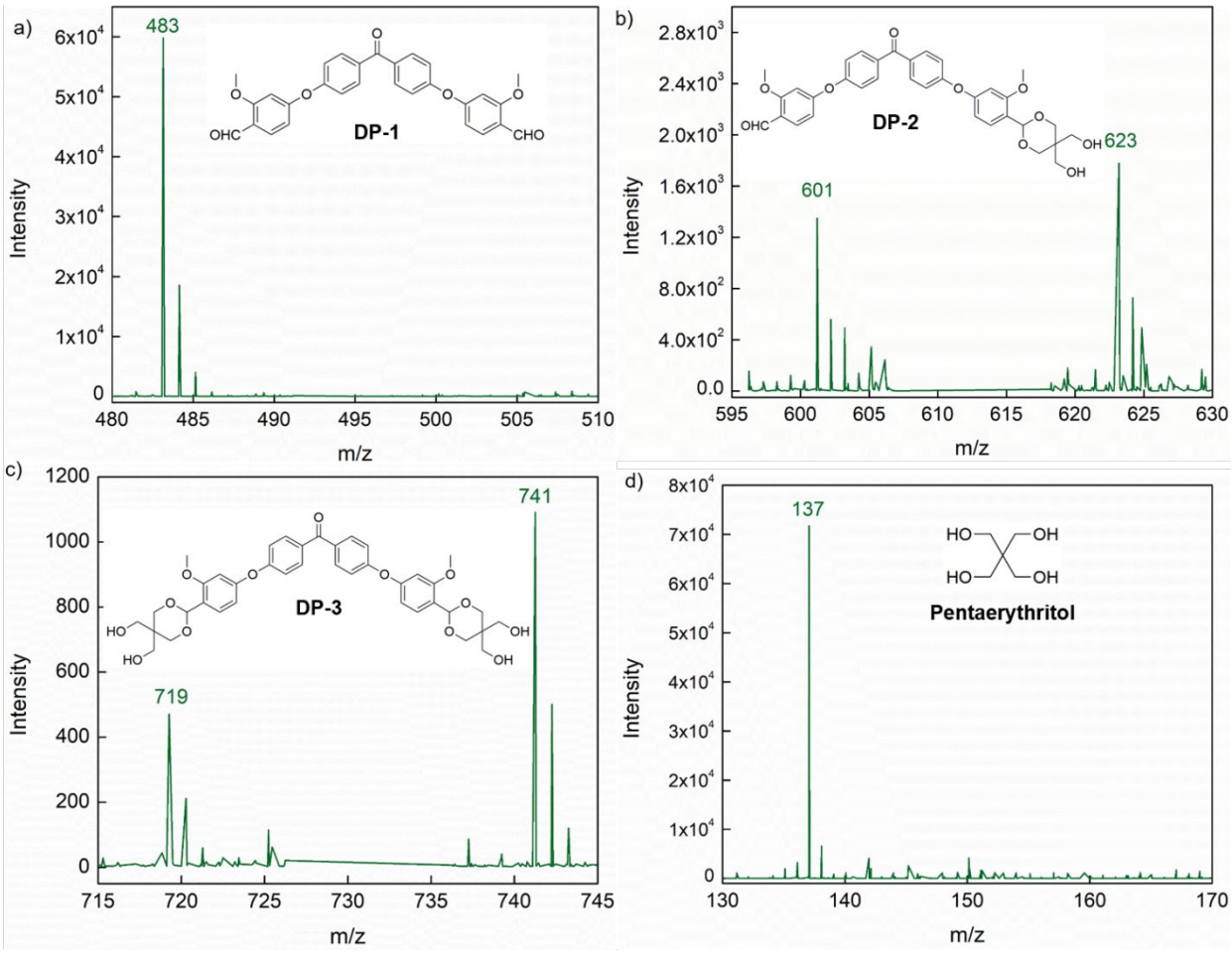

Figure 6: LC-MS data obtained from degradation products of VPA-DFP in *d*-acetone/HCl (0.1 M HCl, pH 1) at room temperature after 24 h degradation time: (a) DP-1, (b) DP-2, (c) DP-3, and (d) pentaerythritol. Degradation experiments were conducted in 0.6 mL *d*-acetone containing 5 µL of 35 wt% aqueous HCl solution.

Table 3: Molecular weight of degradation products, with bound H^+ and Na^+, and m/z observed in LC-MS.

Degradation Product	Molecular Weight (g/mol)	Molecular Weight with bound H^+ (g/mol)	Molecular Weight with bound Na^+ (g/mol)	m/z observed in LC-MS (g/mol)
DP-1	482.1	483.1	505.1	483.1
DP-2	600.2	601.2	623.2	601.2/623.2
DP-3	718.3	719.3	741.3	719.3/741.3
Pentaerythritol	136.1	137.1	159.1	137.1

3.4 Monitoring Time-Evolution of Degradation Product Compositions of VPA-DFP in Acidic d-Acetone

The time-evolution of the degradation product composition was monitored for VPA-DFP in acidic *d*-acetone, using ^{1}H NMR and GPC. As VPA-DFP is not soluble in *d*-acetone, no peaks were observed for the non-degraded polymer and thus observed peaks are associated with the small molecule degradation products (DP-1, DP-2, DP-3, and pentaerythritol), as well as possibly oligomers small enough to be solubilized. As degradation proceeded, peaks associated with the degradation products appeared in the spectra: -CHO (10.01 ppm) of fully hydrolyzed acetals on DP-1 and DP-2, protons of partially hydrolyzed acetals on DP-2 and DP-3 (-CH at 5.48 and 5.58 ppm and -CH_2 in the range of 3.8 ppm to 4.2 ppm), and aromatic protons found on DP-1, DP-2 and DP-3 (6.9-7.8 ppm) (**Figure 7**). The intensities of these peaks increased over the first 10 h and subsequently no further changes were observed, even up to 96 h.

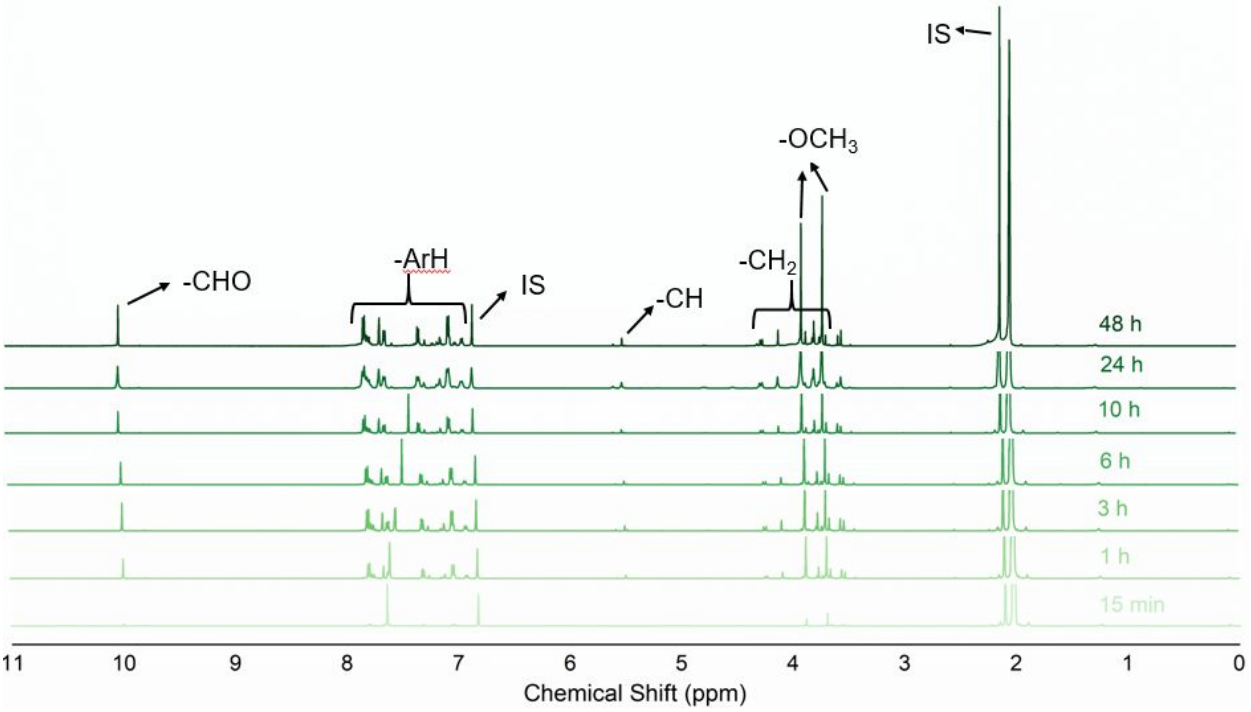

Figure 7: ^{1}H NMR data obtained from the acid-catalyzed hydrolysis of VPA-DFP in *d*-acetone/HCl (0.1 M HCl, pH 1) at room temperature at different time points. Degradation experiments were conducted in 0.6 mL *d*-acetone containing 5 µL of 35 wt% aqueous HCl solution. Labeled on the spectra are the following peaks that were monitored over time: -CHO peaks at 10.01 ppm associated with fully hydrolyzed acetals on DP-1 and DP-2, -CH peaks at 5.48 and 5.58 ppm associated with partially hydrolyzed acetals on DP-2 and DP-3, and aromatic protons (ArH) in the region of 6.9-7.8 ppm, associated with DP-1, DP-2, and DP-3. Additionally, $-CH_2$, $-OCH_3$, and internal standard (IS) peaks are labeled, though their time-dependence was not quantified. A more completely labeled spectrum obtained at 24 h of degradation time is provided in Figure 5.

At early times (i.e. 15 min and beyond), both -CHO (10.01 ppm) and -CH peaks (5.48 and 5.58 ppm) peaks are observed, indicating that both fully and partially hydrolyzed structures are present as soon as the degradation process commences. As the degradation process proceeded, the intensity of the -CHO peak increased drastically, suggesting more acetals were fully hydrolyzed. However, even at long times, when changes in the NMR spectra were no longer observed (i.e. longer than 10 hours), -CH peaks are still observed associated with the partially hydrolyzed acetals. Though the degradation process was not complete, no further changes were observed in the spectra upon continued exposure to the acidic solution. Thus, we suggest that degradation products DP-1,

DP-2, and DP-3 were present at all times during the process, though the majority of the final degradation product mixture was composed of DP-1 (and possibly oligomers with the same end-functionality) and pentaerythritol.

In order to quantify the degradation process further, we monitored changes in concentration of characteristic chemical groups over time with the use of an internal standard (**Figure 8**): -CHO (10.01 ppm, associated with DP-1 and DP-2), cycloacetal -CH (5.48 and 5.58 ppm, associated with DP-2 and DP-3), and aromatic protons (6.9-7.8 ppm, associated with DP-1, DP-2, and DP-3). As oligomers may be present with the same functional end-groups as DP-1, DP-2, and DP-3, we do not attempt to quantify the concentration of each small molecule degradation product, but rather quantify concentrations of each of the relevant functional groups. The concentration of -CHO groups increased rapidly in the first 10 h of degradation time and then exhibited a plateau after 10 h (**Figure 8a**). If all of the polymer were converted to DP-1, the concentration of -CHO would be 0.0279 mol/L under the conditions used in this experiment. However, the plateau concentration of -CHO group was slightly lower, 0.0210 mol/L, due to the presence of partially degraded products DP-2 and DP-3. Similarly, the concentration of -CH groups increased during the first 10 h of degradation time, and then exhibited a relatively constant value of 0.00474 mol/L thereafter, indicating a persistent and unchanging presence of the partially hydrolyzed DP-2 and DP-3 at long times as minority components of the degradation product mixture. Additionally, we monitored the change in concentration of aromatic protons over time (**Figure 8b**). Initially, the polymer was not soluble in acetone and aromatic protons were not observed. However, as the polymer degraded to smaller (possibly oligomeric) molecules, their solubility likely increased. Degradation products DP-1, DP-2 and DP-3 are all fully soluble in acetone and contain the same aromatic protons as the polymer repeat unit structure (**Scheme 3**). If the polymer degraded completely to fully soluble

species (DP-1, DP-2, DP-3, and even oligomers), the final concentration of aromatic protons would have been 0.195 mol/L. We observed an increase in aromatic proton concentration within 10 hours of degradation time, and a plateau value of 0.194 mol/L, consistent with our expectation.

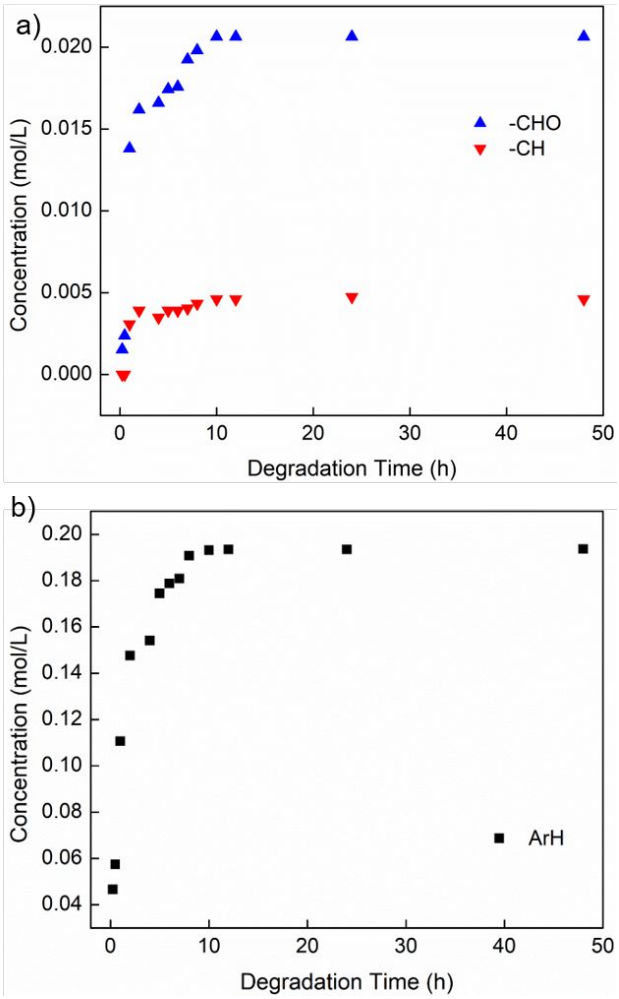

Figure 8: Concentration of (a) -CHO (10.01 ppm) and -CH (5.48 and 5.58 ppm) groups and (b) aromatic protons (6.9-7.8) observed at different time points during VPA-DFP degradation in *d*-acetone/HCl at room temperature, quantified from data in Figure 7.

To further confirm the existence of DP-1, DP-2, DP-3 and oligomeric degradation products, we used GPC to analyze the molecular weight distribution of degradation products at different degradation times (**Figure 9a, Table S1**). The M_n of VPA-DFP prior to degradation was

characterized to be 7.3 kg/mol. After 0.5 h of degradation, the polymer peak shifted substantially to the right, consistent with a molecular weight of around 3 kg/mol. This may be due to the formation of oligomeric degradation products. VPA-DFP is a glassy, semi-crystalline polymer and therefore visually is a white, rigid solid. After 0.5 h of degradation time, it transitioned to a light yellow, soft solid, observed as oligomeric species by GPC. We also noticed the appearance of several lower molecular weight peaks (around 27.2, 27.7, 28.8 and 30.1 min retention time), confirming the presence of smaller degradation products. The molecular weights of smaller species were reasonably consistent with that of DP-3, DP-2, DP-1 and pentaerythritol, respectively (**Table S1**; note that polystyrene standards were used in GPC analyses and therefore only a relative comparison of molecular weights can be made). As the intensities of the peaks associated with the small degradation products increased over time, that of the oligomeric species decreased, indicating further break down of oligomers to DP-1, DP-2, DP-3 and pentaerythritol. We note that at 24 h of degradation time, a small fraction of oligomers still remained. We then varied the molarity of HCl (0.1 – 1 M) at 24 h of degradation time, to explore further degradation of the oligomers at higher acid concentration (**Figure 9b**). We observed the further disappearance of oligomers as the acid concentration was increased, as well as decrease in concentrations of DP-2 and DP-3 and increase in concentration of DP-1 (the fully hydrolyzed byproduct). We did not observed an increase in pentaerythritol concentration as the acid molarity was increased, but we attribute this to the limited solubility of pentaerythritol in DMF (the solvent for GPC experiments).

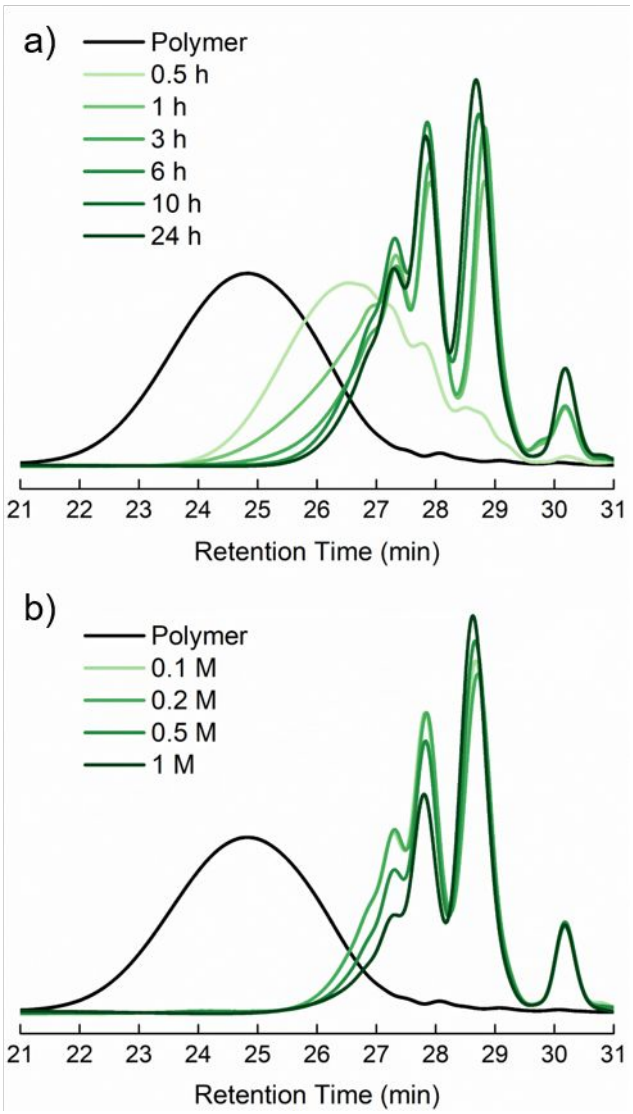

Figure 9: GPC data obtained from degradation products of the acid-catalyzed hydrolysis at room temperature of VPA-DFP in *d*-acetone/HCl: a) 0.1 M HCl (pH 1 at different degradation times and b) varying molarity of acid at 24 h degradation time.

3.5 Impact on Solvent Type on VPA-DFP Degradation Rate

We also compared the degradation rates of VPA-DFP in other solvent systems (acidic *d*-DMSO and D_2O, **Figure 10**). We monitored the change of concentration of -CHO group and we found there was little degradation in D_2O observed up to 168 h, and significantly slower degradation in acidic *d*-DMSO as compared to that observed in in acidic *d*-acetone. Interestingly, while VPA-DFP is insoluble in acetone and water, it is fully soluble in DMSO.

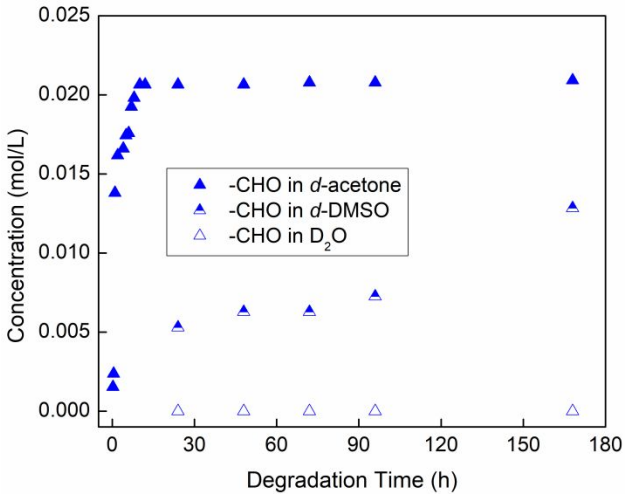

Figure 10: Concentration of -CHO (10.01 ppm) group observed at different time points during VPA-DFP degradation in various solvent systems (*d*-acetone/HCl, *d*-DMSO/HCl and D_2O/HCl, containing 0.1 M HCl). Degradation experiments were conducted in 0.6 mL solvent (*d*-acetone, *d*-DMSO or D_2O) containing 5 µL of 35 wt% aqueous HCl solution.

Variation of the solvent composition impacts two important factors which influence the hydrolysis rate:[16] the affinity of the polymer to the solvent and the solubility of the degradation products. We measured the contact angles of a VPA-DFP coated silicon wafer in various solvents (acidic *d*-acetone, acidic *d*-DMSO, and acidic D_2O) and they are summarized in **Table 4**. VPA-DFP exhibited the lowest contact angle in acidic *d*-acetone, followed by acidic *d*-DMSO, and the highest contact angle in D_2O. The rate of hydrolysis therefore appears correlated with the solvent affinity of the polymer.

We also calculated the Hansen Solubility Parameters (δ) of the four degradation products (described in ESI and summarized in **Table 5**). We found that δ of DP-1 is very similar to that of *d*-DMSO, and δ of DP-3 and pentaerythritol were very similar to that of D_2O, which should be an indicator of the most favorable conditions for solubility. δ of DP-2 was not close to any one solvent, indicating conditions were not particularly favorable for solubility. Importantly, δ of all four degradation products were most dissimilar to that of acidic acetone, indicating the worse

conditions for solubility in this solvent. Therefore, we observe no correlations between the predicted degradation product solubilities and observed rates of hydrolysis, indicating the solvent affinity of the polymer is likely a more important factor governing the rate of hydrolysis.

Table 4: Contact angles of VPA-DFP in various solvent systems

Solvent[a]	Contact Angle (°)
Acidic *d*- acetone	9.5 ± 2.7
Acidic *d*-DMSO	14.7 ± 1.6
Acidic D_2O	69.7 ± 0.8

[a] Acidic solvent compositions were identical to that used in degradation experiments

Table 5: Hansen Solubility Parameter (δ) of VPA-DFP degradation products and solvents

Degradation Product or Solvent	δ ($MPa^{1/2}$)
DP-1	27.5
DP-2	36.3
DP-3	48.1
Pentaerythritol	41.2
Acetone	19.9
DMSO	24.4
H_2O	47.8

4. Conclusions

Degradable, thermally stable, and high T_g and T_m polymers were synthesized from bioaromatics, including vanillin and its derivative syringaldehyde, employing difluoro aromatic co-monomers. Incorporation of spiro cycloacetal units, along with aromatic groups, into the polymer backbone resulted in high thermal degradation temperatures, as well as high T_g and T_m. The presence of labile spiro cycloacetal units provided a mechanism for degradation under acid-

catalyzed hydrolysis. Degradation studies indicated these spiro cycloacetal units were relatively stable in an acidic aqueous medium (pH ~ 1), but could be degraded in acidic organic solvents (DMSO and acetone). Among the various solvents, degradation occurred most rapidly in acidic acetone. Four small molecule degradation products, along with solubilized oligomers, were detected in the degradation solution, produced through the acid-catalyzed cleavage of acetal groups. The solvent affinity of the polymer was identified to be a more important factor governing the rate of hydrolysis than the predicted degradation product solubilities.

Acknowledgements

The authors would like to thank Scott K. Smith for access and training in the University of Houston Department of Chemistry Nuclear Magnetic Resonance Facility. We thank Ramanan Krishnamoorti and Tzu-Han Li for access to and training on the TGA instrument. We thank Eva Harth and Anthony Keyes for contributing GPC analyses. We thank Alamgir Karim and Stephanie Sontgerath for access to and assistance with flow coating. We also thank Stacey Louie and Charisma Lattao for access to and assistance with LC-MS. This work is in support of ONR-Code 30 OTA #N00014-18-9-0001.This material is based upon work supported by the National Science Foundation under Grant No. DMR-1611376.

References

1. Hillmyer, M. A., The promise of plastics from plants. *Science* **2017,** *358* (6365), 868-870.
2. Hufendiek, A.; Lingier, S.; Du Prez, F. E., Thermoplastic polyacetals: chemistry from the past for a sustainable future? *Polymer Chemistry* **2019,** *10* (1), 9-33.
3. Wang, Z.; Yuan, L.; Tang, C., Sustainable Elastomers from Renewable Biomass. *Acc. Chem. Res.* **2017,** *50* (7), 1762-1773.
4. Miller, S. A., Sustainable Polymers: Opportunities for the Next Decade. *ACS Macro Letters* **2013,** *2* (6), 550-554.
5. Zhu, Y.; Romain, C.; Williams, C. K., Sustainable polymers from renewable resources. *Nature* **2016,** *540* (7633), 354-362.
6. Cao, H.; Rupar, P. A., Recent Advances in Conjugated Furans. *Chemistry – A European Journal* **2017,** *23* (59), 14670-14675.
7. Gandini, A.; Lacerda, T. M.; Carvalho, A. J. F.; Trovatti, E., Progress of Polymers from Renewable Resources: Furans, Vegetable Oils, and Polysaccharides. *Chemical Reviews* **2016,** *116* (3), 1637-1669.
8. Sheldon, R. A., Green and sustainable manufacture of chemicals from biomass: state of the art. *Green Chemistry* **2014,** *16* (3), 950-963.
9. Llevot, A.; Dannecker, P.-K.; von Czapiewski, M.; Over, L. C.; Söyler, Z.; Meier, M. A. R., Renewability is not Enough: Recent Advances in the Sustainable Synthesis of Biomass-Derived Monomers and Polymers. *Chemistry – A European Journal* **2016,** *22* (33), 11510-11521.
10. Jambeck, J. R.; Geyer, R.; Wilcox, C.; Siegler, T. R.; Perryman, M.; Andrady, A.; Narayan, R.; Law, K. L., Plastic waste inputs from land into the ocean. *Science* **2015,** *347* (6223), 768.
11. Geyer, R.; Jambeck, J. R.; Law, K. L., Production, use, and fate of all plastics ever made. *Science Advances* **2017,** *3* (7), e1700782.
12. Albertsson, A.-C.; Hakkarainen, M., Designed to degrade. *Science* **2017,** *358* (6365), 872.
13. Hillmyer, M. A.; Tolman, W. B., Aliphatic Polyester Block Polymers: Renewable, Degradable, and Sustainable. *Accounts of Chemical Research* **2014,** *47* (8), 2390-2396.
14. Lavilla, C.; Alla, A.; Martínez de Ilarduya, A.; Benito, E.; García-Martín, M. G.; Galbis, J. A.; Muñoz-Guerra, S., Biodegradable aromatic copolyesters made from bicyclic acetalized galactaric acid. *Journal of Polymer Science Part A: Polymer Chemistry* **2012,** *50* (16), 3393-3406.
15. Ying, H.; Cheng, J., Hydrolyzable Polyureas Bearing Hindered Urea Bonds. *Journal of the American Chemical Society* **2014,** *136* (49), 16974-16977.
16. Shen, M.; Cao, H.; Robertson, M. L., Hydrolysis and Solvolysis as Benign Routes for the End-of-Life Management of Thermoset Polymer Waste. *Annual Review of Chemical and Biomolecular Engineering* **2020,** *11* (1), 183-201.
17. Shen, M.; Robertson, M. L., Degradation Behavior of Biobased Epoxy Resins in Mild Acidic Media. *ACS Sustainable Chemistry & Engineering* **2021,** *9* (1), 438-447.
18. Vijjamarri, S.; Hull, M.; Kolodka, E.; Du, G., Renewable Isohexide-Based, Hydrolytically Degradable Poly(silyl ether)s with High Thermal Stability. *ChemSusChem* **2018,** *11* (17), 2881-2888.
19. Tschan, M. J. L.; Brulé, E.; Haquette, P.; Thomas, C. M., Synthesis of biodegradable polymers from renewable resources. *Polymer Chemistry* **2012,** *3* (4), 836-851.
20. Nakajima, H.; Dijkstra, P.; Loos, K., The Recent Developments in Biobased Polymers toward General and Engineering Applications: Polymers that are Upgraded from Biodegradable

Polymers, Analogous to Petroleum-Derived Polymers, and Newly Developed. *Polymers* **2017,** *9* (10), 523.
21. Pemba, A. G.; Flores, J. A.; Miller, S. A., Acetal metathesis polymerization (AMP): A method for synthesizing biorenewable polyacetals. *Green Chemistry* **2013,** *15* (2), 325-329.
22. Samanta, S.; Bogdanowicz, D. R.; Lu, H. H.; Koberstein, J. T., Polyacetals: Water-Soluble, pH-Degradable Polymers with Extraordinary Temperature Response. *Macromolecules* **2016,** *49* (5), 1858-1864.
23. Andrade-Gagnon, B.; Bélanger-Bouliga, M.; Trang Nguyen, P.; Nguyen, T. H. D.; Bourgault, S.; Nazemi, A., Degradable Spirocyclic Polyacetal-Based Core-Amphiphilic Assemblies for Encapsulation and Release of Hydrophobic Cargo. *Nanomaterials* **2021,** *11* (1), 161.
24. Elling, B. R.; Su, J. K.; Xia, Y., Degradable Polyacetals/Ketals from Alternating Ring-Opening Metathesis Polymerization. *ACS Macro Letters* **2020,** *9* (2), 180-184.
25. Moreno, A.; Lligadas, G.; Ronda, J. C.; Galià, M.; Cádiz, V., Orthogonally functionalizable polyacetals: a versatile platform for the design of acid sensitive amphiphilic copolymers. *Polymer Chemistry* **2019,** *10* (38), 5215-5227.
26. Paramonov, S. E.; Bachelder, E. M.; Beaudette, T. T.; Standley, S. M.; Lee, C. C.; Dashe, J.; Fréchet, J. M. J., Fully Acid-Degradable Biocompatible Polyacetal Microparticles for Drug Delivery. *Bioconjugate Chemistry* **2008,** *19* (4), 911-919.
27. Rajput, B. S.; Gaikwad, S. R.; Menon, S. K.; Chikkali, S. H., Sustainable polyacetals from isohexides. *Green Chemistry* **2014,** *16* (8), 3810-3818.
28. Debsharma, T.; Yagci, Y.; Schlaad, H., Cellulose-Derived Functional Polyacetal by Cationic Ring-Opening Polymerization of Levoglucosenyl Methyl Ether. *Angewandte Chemie International Edition* **2019,** *58* (51), 18492-18495.
29. Fache, M.; Boutevin, B.; Caillol, S., Vanillin, a key-intermediate of biobased polymers. *European Polymer Journal* **2015,** *68*, 488-502.
30. Fache, M.; Darroman, E.; Besse, V.; Auvergne, R.; Caillol, S.; Boutevin, B., Vanillin, a promising biobased building-block for monomer synthesis. *Green Chemistry* **2014,** *16* (4), 1987-1998.
31. Ma, S.; Wei, J.; Jia, Z.; Yu, T.; Yuan, W.; Li, Q.; Wang, S.; You, S.; Liu, R.; Zhu, J., Readily recyclable, high-performance thermosetting materials based on a lignin-derived spiro diacetal trigger. *Journal of Materials Chemistry A* **2019,** *7* (3), 1233-1243.
32. Pemba, A. G.; Rostagno, M.; Lee, T. A.; Miller, S. A., Cyclic and spirocyclic polyacetal ethers from lignin-based aromatics. *Polymer Chemistry* **2014,** *5* (9), 3214-3221.
33. Nguyen, H. T. H.; Qi, P.; Rostagno, M.; Feteha, A.; Miller, S. A., The quest for high glass transition temperature bioplastics. *Journal of Materials Chemistry A* **2018,** *6* (20), 9298-9331.
34. Labadie, J. W.; Hedrick, J. L.; Ueda, M., Poly(aryl ether) Synthesis. In *Step-Growth Polymers for High-Performance Materials*, American Chemical Society: 1996; Vol. 624, pp 210-225.
35. Lindström, A.; Hakkarainen, M., Designed Chain Architecture for Enhanced Migration Resistance and Property Preservation in Poly(vinyl chloride)/Polyester Blends. *Biomacromolecules* **2007,** *8* (4), 1187-1194.
36. Park, S.-A.; Jeon, H.; Kim, H.; Shin, S.-H.; Choy, S.; Hwang, D. S.; Koo, J. M.; Jegal, J.; Hwang, S. Y.; Park, J.; Oh, D. X., Sustainable and recyclable super engineering thermoplastic from biorenewable monomer. *Nature Communications* **2019,** *10* (1), 2601.

37. Chung, I. S.; Kim, S. Y., Meta-Activated Nucleophilic Aromatic Substitution Reaction: Poly(biphenylene oxide)s with Trifluoromethyl Pendent Groups via Nitro Displacement. *Journal of the American Chemical Society* **2001,** *123* (44), 11071-11072.
38. Jedeon, K.; De la Dure-Molla, M.; Brookes, S. J.; Loiodice, S.; Marciano, C.; Kirkham, J.; Canivenc-Lavier, M.-C.; Boudalia, S.; Bergès, R.; Harada, H.; Berdal, A.; Babajko, S., Enamel Defects Reflect Perinatal Exposure to Bisphenol A. *The American Journal of Pathology* **2013,** *183* (1), 108-118.
39. Klein, R.; Schüll, C.; Berger-Nicoletti, E.; Haubs, M.; Kurz, K.; Frey, H., ABA Triblock Copolymers Based on Linear Poly(oxymethylene) and Hyperbranched Poly(glycerol): Combining Polyacetals and Polyethers. *Macromolecules* **2013,** *46* (22), 8845-8852.
40. Hammami, N.; Majdoub, M.; Habas, J.-P., Structure-properties relationships in isosorbide-based polyacetals: Influence of linear or cyclic architecture on polymer physicochemical properties. *European Polymer Journal* **2017,** *93*, 795-804.
41. Chikkali, S.; Stempfle, F.; Mecking, S., Long-Chain Polyacetals From Plant Oils. *Macromolecular Rapid Communications* **2012,** *33* (13), 1126-1129.
42. Ortmann, P.; Heckler, I.; Mecking, S., Physical properties and hydrolytic degradability of polyethylene-like polyacetals and polycarbonates. *Green Chemistry* **2014,** *16* (4), 1816-1827.
43. Law, A. C.; Stankowski, D. S.; Bomann, B. H.; Suhail, S.; Salmon, K. H.; Paulson, S. W.; Carney, M. J.; Robertson, N. J., Synthesis and material properties of elastomeric high molecular weight polycycloacetals derived from diglycerol and meso-erythritol. *Journal of Applied Polymer Science* **2020,** *137* (23), 48780.
44. Rostagno, M.; Price, E. J.; Pemba, A. G.; Ghiriviga, I.; Abboud, K. A.; Miller, S. A., Sustainable polyacetals from erythritol and bioaromatics. *Journal of Applied Polymer Science* **2016,** *133* (45).
45. Sonmez, H. B.; Kuloglu, F. G.; Karadag, K.; Wudl, F., Terephthalaldehyde- and isophthalaldehyde-based polyspiroacetals. *Polymer Journsal* **2012,** *44* (3), 217-223.